Nanoscale

Accepted Manuscript

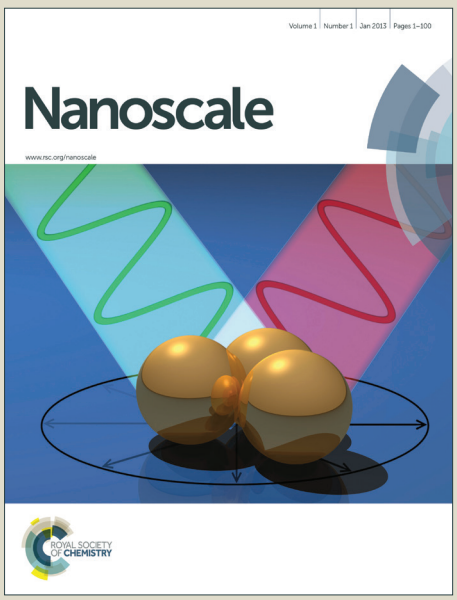

ROYAL SOCIETY OF CHEMISTRY

www.rsc.org/nanoscale

Nanoscale

RSCPublishing

COMMUNICATION

Direct Electrochemical and AFM Detection of Amyloid-β Peptide Aggregation on Basal Plane HOPG

Cite this: DOI: 10.1039/x0xx00000x

Received 00th January 2012,
Accepted 00th January 2012

DOI: 10.1039/x0xx00000x

www.rsc.org/

Paula Lopes,[a,b] Meng Xu,[c] Min Zhang[c], Ting Zhou[c], Yanlian Yang[c]*, Chen Wang[c] and Elena E. Ferapontova[a,b]*

Amyloidogenesis is associated with more than 30 human diseases, including Alzheimer's one related to aggregation of β-amyloid peptide (Aβ). Here, consecutive stages of Aβ42 aggregation and amyloid fibril formation were followed electrochemically *via* oxidation of tyrosines (Tyr) in Aβ42 adsorbed on the basal plane graphite electrode and directly correlated with Aβ42 morphological changes observed by atomic force microscopy at the same substrate. The results offer new tools for analysis of mechanisms of Aβ aggregation.

Over 30 human diseases are now related to amyloidogenesis, the formation of aggregated β-sheet polypeptide structures that appear as water-insoluble deposits of amyloid fibrils.[1] Among examples of localized amyloidosis in the brain is Alzheimer's disease (AD) associated with the formation of neurotic plaques composed of extracellular deposits of self-aggregating β-amyloid peptide (Aβ) of 39-42-residues in length.[1] Genetic and biomarker studies of AD genesis[2,3] indicate that it is mostly due to imbalance in the production and clearance of Aβ followed by its aggregation in the brain, Aβ42 being the major component of amyloid plaque deposits.[4] It exhibits lower solubility and has the propensity to form proto-fibrils and fibrillar aggregates at lower concentrations and higher rates than other Aβ variants.[5,6] Around 4 kDa in weight, Aβ42 contains both hydrophilic N-terminus and hydrophobic C-terminus regions (Figure 1). In its native form, Aβ42 is unfolded (α-helix or random coil), but under various fibrillization conditions aggregates into a β-sheet structure composed of several β-sheet layers of ordered fibrils.[7] Though molecular mechanisms of fibrillization are not completely clear, it is known to be a multi-step nucleated polymerrization[8-10] that involves soluble oligomeric inter-mediates of different size and forms.[11] These pre-fibrillar β-aggregates were reported to be more neurotoxic than both monomeric Aβ and mature amyloid fibrils.[12,13]

It however still remains uncertain which specific aggregates (protofibrils, protofilaments or oligomers) are most toxic,[13,14] and further studies of amyloidogenesis and dynamics of formation of prefibrillar intermediates, including their precise identification, are crucial for understanding the routes of AD pathogenesis. That requires fast and dynamic diagnostic tools for analysis of kinetics of aggregation, in order to monitor disease progression and its possible treatments.[16-19] Aβ aggregation *in vitro* is commonly studied by such techniques as circular dichroism (CD) spectroscopy, fluorescence spectroscopy, and electron and atomic force microscopy (EM and AFM). In particular, detection of Aβ aggregation and plaque formation by thioflavin T (ThT) and its derivatives

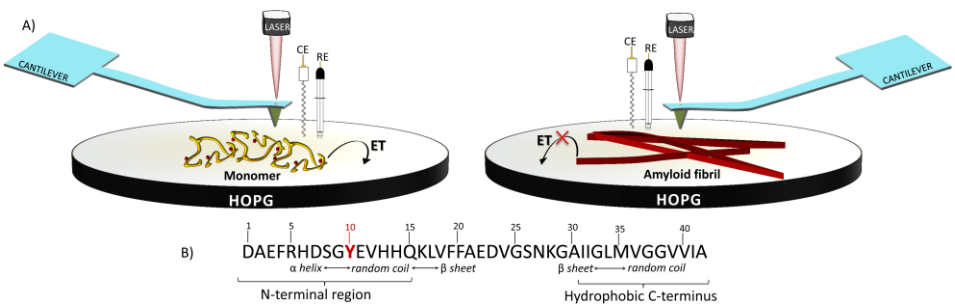

Figure 1. (A) Schematic representation of the electrochemical and AFM assay of Aβ42 aggregation on the surface of basal plane HOPG working as an electrode in electrochemistry and as a substrate in AFM studies; RE and CE are reference and counter electrodes, respectively. (B) Amino acid sequence of the Aβ42 monomer (PDB ID:1Z0Q)[15].

specifically interacting with fibrils has become a reference method.[20] Along with that, electrochemical methods can successfully compete with other techniques in analysis of protein conformational changes either by addressing their bioelectrocatalytic activity[21,22] or by monitoring electrochemical oxidation of their surface amino-acid residues such as tyrosine (Tyr), tryptophan, and cystine/cysteine.[23-28] In particular, aggregation of Aβ was shown to affect the electrochemical accessibility of its single Tyr residue (Figure 1B) thus enabling electrochemical monitoring of Aβ fibrillization.[29] In this pioneer work, electrooxidation of diffusing in solution Aβ was followed at glassy carbon and Tyr oxidation signals were correlated with the ThT fluorescence and AFM imaging on mica, bare and modified with 3-(aminopropyl)-triethoxysilane. Therewith, significant morphological differences in the shape of Aβ aggregates were observed on bare and modified mica,[29] pointing out the important effect of the substrate nature on the conformational state and thus electrochemistry of peptides.

For robust screening of amyloidosis, electrochemical and surface studies should be unambiguously correlated with each other. Here, different steps of Aβ42 peptide aggregation, from monomers to mature amyloid fibrils, were monitored by electrochemical oxidation of Tyr of Aβ42 adsorbed on the basal plane of highly oriented pyrolytic graphite (HOPG) and via AFM studies of Aβ42 on the same substrate (Figure 1). We aimed at the development of advanced tools for analysis of mechanism and kinetics of Aβ aggregation *in vitro*.

Electrochemical oxidation of Aβ42 adsorbed on the HOPG electrodes was followed by differential pulse voltammetry (DPV). Although Aβ42 contains only one Tyr residue at position 10 (Figure 1B), its oxidation gave rise to a well-defined peak at 640±7 mV (Figure 2) consistent with electrooxidation of its Tyr.[28] The dependence of the Tyr oxidation current, I, on the concentration of adsorbed Aβ42, $C_{A\beta}$, followed a Langmuir isotherm with a saturation level reached at peptide concentrations exceeding 450 μM (Figure 2 inset):

$$I = I_{max} \times K \times C_{A\beta} / (1 + K \times C_{A\beta}) \quad (1)$$

The maximal current I_{max} of 0.30±0.02 μA corresponded to 1.75±0.09 pmoles of electroactive Aβ42 (calculated in assumption of $1e^-$ electrooxidation of a single Aβ42 Tyr)[28] consistent with a protein monolayer coverage of 15.9±0.8 pmol cm^{-2} and a protein footprint of around 10 nm^2. This footprint correlates with the unfolded Aβ42 structure (4.2 nm×2.3 nm in its largest dimensions)[15] then occupying a surface space of ca. 9.7 nm^2. Such loosely packed monolayer is quite different from very compact films produced by another amyloidosis-related protein, alpha-synuclein (αSN), on spectroscopic graphite[28] and is consistent with a weaker adsorption of Aβ42 on HOPG (ESI): the equilibrium constant K reflecting the relationship between the Aβ42 adsorption-desorption constants (0.006± 0.001) is much lower than the 0.17±0.03 value observed for αSN.

Aβ42 aggregation was then electrochemically monitored with 125 μM peptide (unsaturated adsorption conditions, ESI) in a 20 mM phosphate buffer solution containing 0.15 M NaCl (PBS), pH 7, for different times of Aβ42 incubation at 37°C (ESI). With increasing incubation time the Tyr oxidation signal gradually decreased and the peak potential shifted to less positive values (Figure 3B, Table 1) until the signal became undistinguishable from the background one (after 48 h). Suppressed Tyr signals in aggregated Aβ42 adsorbed on HOPG were consistent with a smaller number of Tyr residues exposed to the electrode surface and thus available for electrooxidation. Based on electro-chemical signals, several stages of aggregation affecting Tyr availability might be expected: the initial stage, when monomers undergo an α-helix to β-sheet transition and self-associate forming soluble dimers and insoluble oligomers (multistep nucleation-aggregation), and consecutive stages of oligomer and proto-fibril bidirectional elongation until Tyr becomes finally totally hidden inside the fibrils.[30,31]

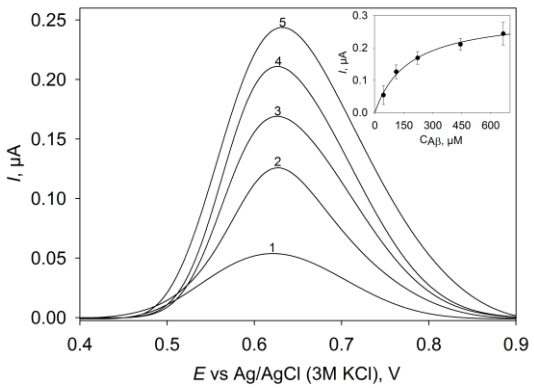

Figure 2. Representative DPVs of Aβ42 adsorbed on the HOPG electrode, concentrations: (1) 44, (2) 111, (3) 222, (4) 443, and (5) 665 μM Aβ42. DPV (recorded in PBS, pH 7): potential step 10 mV, amplitude 25 mV, pulse time 50 ms; apparent scan rate 20 mV s^{-1}. Inset: Dependence of the Tyr oxidation peak current, I, on the Aβ42 concentration. The solid line is fitting to the Langmuir isotherm by the Sigma Plot software (Eq. 1)

AFM imaging of 12 h incubated Aβ42 adsorbed on HOPG revealed homogeneously distributed small globular aggregates (Figure 3A-12h), resulting from basic self-assembly of Aβ42 monomers in more complex structures. Statistical analysis of the particles height distribution gave these globular species diameter of 3-5±0.5 nm, approaching a soluble oligomer size,[32] also shown on mica.[31] Earlier it has been reported that 5 nm globules correspond to the structures containing 6-9 Aβ42 units.[32] Larger aggregates resembling protofibrils as the first fibrillar structures could be further identified for 24 h incubated Aβ42 (Figure 3A-24h). Their length was over 1 μm, with a height of 6.0±1.5 nm consistent with the size of 12 h incubated Aβ42 aggregates thus supporting bidirectional association of oligomers.[31] As a further support for the ability of protofibrils to serve as building blocks for mature fibrils, a few examples of protofibril branching into two and more filaments can be distinguished in Figure 3A-24h (dashed circles). Aggregated entities of variable shapes also can be seen reinforcing the view that Aβ42 fibrillogenesis is a complex process proceeding through multiple steps and pathways. After 36 h incubation

Aβ42 formed fibrils (Figure 3A-36h) with a diameter of 4-8 nm and lengths ranged between 0.5 and 5 μm (some fibrils >5 μm).

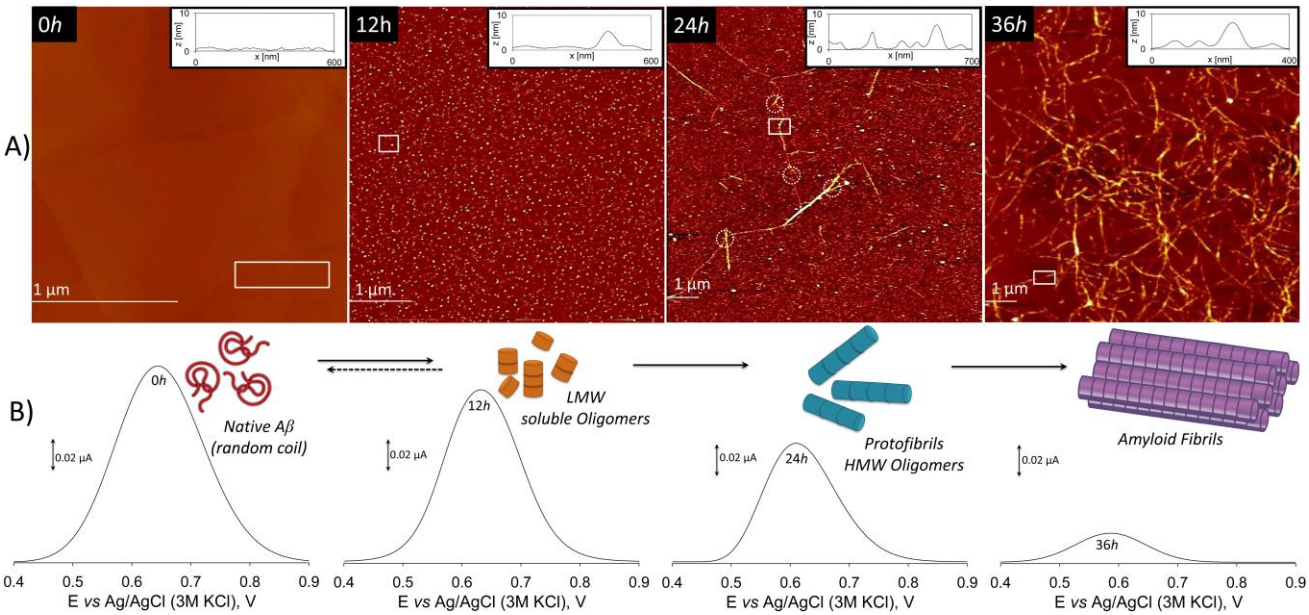

Figure 3. Representative (A) AFM images and (B) baseline-corrected DPVs recorded with Aβ42 adsorbed in its different aggregation states on freshly cleaved HOPG, Aβ42 incubation times: 0, 12, 24 and 36 h (see ESI† for details). (A) Insets: height profiles corresponding to the sections indicated in the images. (B) Insets: schematic representation of the Aβ42 aggregation process (LMW and HMW: low and high molecular weight, correspondingly).

These Aβ42 conformational transitions were electrochemically observed as a concomitant decrease in the Tyr oxidation currents accompanied by the Tyr potential shift to less positive values, consistent with the local polarity changes in the redox species environment[28, 33] (Figure 3, Table 1). After 36 h incubation the Aβ42 Tyr oxidation signal decreased 86%, a residual signal remaining from monomers or LMW aggregates, and no Tyr signal could be detected after 48 h incubation as a result of the complete Aβ42 amyloid fibrillization.

Thus, a direct correlation of Aβ42 surface and electrochemical properties changing in the course of its fibrillization allows one to use the variation in the Tyr redox signal for analysis of the peptide conformational states, particularly pronounced at earlier stages of Aβ42 aggregation (in the context of the particles height profiles, Figure 4). Along with that, electrochemical data on the surface population of Aβ42 monomers concomitantly decreasing during fibrillization as estimated from the DPV peak current intensities[34] (Table 1, see ESI† for details) provide another simple, fast and still efficient tool for analysis of the kinetics of Aβ42 aggregation and fibrillization (Figure 4, inset). If the assumption is made on the existing equilibrium between the electrochemically active monomers and electrochemically mute Aβ42 aggregates on the HOPG surface similar to the one in solution, then different rates of aggregation/fibril formation can be followed for different steps of the fibrillization process, with a maximal rate of monomer aggregation (the fastest Tyr removal from the electrode reaction zone) in-between 24 - 36 h of incubation correlating with a mature fibril formation step as the most rapid compared to the aggregates seeding and proto-fibril formation steps.

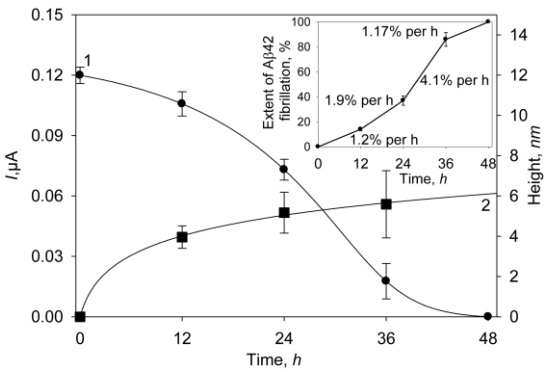

Figure 4. Dependence of the (1) Tyr oxidation current, *I*, (2) oligomers/fibrils AFM height profile, and (inset) extent of Aβ42 fibril formation on the fibrillization time. Inset: for details see ESI†.

To conclude, Aβ42 aggregation and amyloid fibril formation were followed electrochemically *via* oxidation of the Tyr10 residue of Aβ42 adsorbed onto basal plane HOPG displaying inert substrate features. Electrochemical data were for the first time correlated with direct AFM imaging of Aβ42 fibrillization on the same substrate. They evidence that Aβ42 conformational changes during its aggregation can be directly detected by following the electrochemical signal of Tyr oxidation in Aβ42 adsorbed on HOPG that consistently decreases in the course of Aβ42 aggregation. Correlated with the AFM data, electrochemistry of Aβ42 Tyr10 at HOPG provides a simple and sensitive *in vitro* tool for monitoring of Aβ42 aggregation, which allows both kinetic and morphological characterization of the peptide and thus may be used as an advanced screening platform for analysis of aggregation kinetics and drug response, in order to efficiently monitor AD progression and treatments.

Table 1. Some selected characteristics of the AFM and electrochemical analysis of Aβ42 aggregation at basal plane HOPG.

Time-course species	AFM: aggregates height/length (nm)	Oxidation potential of the Tyr residue, E_{ox}, mV,	DPV peak currents, $(I_p)_{max}$, μA	Surface amount of Aβ42 monomers, pmoles [a]	Surface coverage, $\Gamma_{Aβ42}$, pmol cm^{-2} [a]
0 h-Monomer	-	640±4	0.126±0.01	0.73±0.06	6.64±0.55
12 h-Oligomers	3-5±0.5/globular shaped	630±4	0.110±0.01	0.63±0.06	5.72±0.55
24 h-Protofibrils	3-6±1/ >1000	610±5	0.080±0.005	0.46±0.03	4.18±0.27
36 h-Fibrils	5±1/ 500-5000	590±8	0.018±0.005	0.10±0.03	0.91±0.27

[a] Surface amount of monomers was estimated from the DPV peak currents $(I_p)_{max}$ corresponding to the oxidation of Tyr in Aβ42 (see ESI† for details).

Notes and references

[a]Interdisciplinary Nanoscience Center (iNANO), Science and Technology, Aarhus University, Gustav Wieds Vej 1590-14, DK-8000 Aarhus C, Denmark; E-mail: elena.ferapontova@inano.au.dk

[b] Sino-Danish Centre for Education and Research (SDC) at iNANO;

[c] National Center for Nanoscience and Technology, 100190 Beijing, China; E-mail: yangyl@nanoctr.cn

Electronic Supplementary Information (ESI) available: [Experimental details: procedures for Aβ42 aggregation and electrode modification, DPV/AFM measurements and analysis]. See DOI: 10.1039/c000000x/

Acknowledgements: This work was supported by the Sino-Danish Center for Education and Research (SDC), Sino-Danish Joint Program of National Natural Science Foundation of China (21261130090), Aarhus University starting grant to EF and Danish Council for Independent Research, Natural Sciences (FNU), project number 11-107176.

References

1. D. J. Selkoe, Physiolog. Rev., 2001, 81, 741-766.
2. M. P. Lambert, A. K. Barlow, B. A. Chromy, C. Edwards, R. Freed, M. Liosatos, T. E. Morgan, I. Rozovsky, B. Trommer, K. L. Viola, P. Wals, C. Zhang, C. E. Finch, G. A. Krafft and W. L. Klein, Proc. Natl. Acad. Sci. U.S.A., 1998, 95, 6448-6453.
3. S. Gandy, New Eng. J. Med., 2012, 367, 864-866.
4. A. E. Roher, J. D. Lowenson, S. Clarke, A. S. Woods, R. J. Cotter, E. Gowing and M. J. Ball, Proc. Natl. Acad. Sci. U.S.A., 1993, 90, 10836-10840.
5. K. N. Dahlgren, A. M. Manelli, W. B. Stine, L. K. Baker, G. A. Krafft and M. J. LaDu, J. Biol. Chem., 2002, 277, 32046-32053.
6. S. A. Gravina, L. Ho, C. B. Eckman, K. E. Long, L. Otvos, L. H. Younkin, N. Suzuki and S. G. Younkin, J. Biol. Chem., 1995, 270, 7013-7016.
7. G. T. Debelouchina, M. J. Bayro, A. W. Fitzpatrick, V. Ladizhansky, M. T. Colvin, M. A. Caporini, C. P. Jaroniec, V. S. Bajaj, M. Rosay, C. E. MacPhee, M. Vendruscolo, W. E. Maas, C. M. Dobson and R. G. Griffin, J. Am. Chem. Soc., 2013, 135, 19237-19247.
8. C. M. Dobson, TiBS, 1999, 24, 329-332.
9. K. Garai, B. Sahoo, P. Sengupta and S. Maiti, J. Chem. Phys., 2008, 128, 045102-045107.
10. D. Kashchiev, S. Auer, J. Chem. Phys., 2010, 132, 215101-215110.
11. A. Jan, D. M. Hartley and H. A. Lashuel, Nat. Neurosci., 2010, 5, 1186-1209.
12. I. Benilova, E. Karran and B. De Strooper, Nat. Neurosci., 2012, 15, 349-357.
13. M. Stefani and C. M. Dobson, J Mol Med, 2003, 81, 678-699.
14. B. Keshet, I. H. Yang and T. A. Good, Biotechnol. Bioeng., 2010, 106, 333-337.
15. S. Tomaselli, V. Esposito, P. Vangone, N. A. van Nuland, A. M. Bonvin, R. Guerrini, T. Tancredi, P. A. Temussi and D. Picone, ChemBioChem, 2006, 7, 257-267
16. X. Ma, L. Liu, X. Mao, L. Niu, K. Deng, W. Wu, Y. Li, Y. Yang and C. Wang, J. Mol. Biol., 2009, 388, 894-901.
17. K. Ono, Y. Yoshiike, A. Takashima, K. Hasewaga, H. Naiki and M. Yamada, J. Neurochem., 2003, 87, 172.
18. Z. Szabo, E. Klement, K. Jost, M. Zarandi, K. Soos and B. Penke, Biochem. Biophys. Res. Commun., 1999, 265, 297.
19. Y. Yoshiike, K. Tanemura, O. Murayama, T. Akagi, M. Murayama, S. Sata, X. Sun, N. Tanaka and A. Takashima, J. Biol. Chem., 2001, 276, 32293.
20. W. E. Klunk, Y. Wang, G. Huang, M. L. Debnath, D. P. Holt, L. Shao, R. L. Hamilton, M. D. Ikonomovic, S. T. DeKosky and C. A. Mathis, J. Neurosci., 2003, 23, 6.
21. E. E. Ferapontova, in Encyclopedia of Sensors, eds. C. A. Grimes, E. C. Dickey and M. V. Pishko, American Scientific Publishers, Stevenson Ranch, California, USA, 2006, pp. 391-422.
22. A. V. Kartashov, G. Serafini, M. Dong, S. Shipovskov, I. Gazaryan, F. Besenbacher and E. E. Ferapontova, Phys. Chem. Chem. Phys., 2010, 12, 10098-10107.
23. V. Barbec and V. Mornstein, Biophys. Chem., 1980, 12, 159.
24. J. A. Reynaud, B. Malfoy and A. Bere, J. Electroanal. Chem., 1980, 116, 595.
25. X. Cai, G. Rivas, P. A. M. Farias, H. Shiraishi, J. Wang and E. Palecek, Anal. Chim. Acta, 1996, 332, 49.
26. A. Lokszteijn, W. Dzwolak and P. Krysinski, Bioelectrochem., 2008, 72, 34-40.
27. V. W.-S. Hung, H. Masoom and K. Kerman, J. Electroanal. Chem., 2012, 681, 89-95.
28. P. Lopes, H. Dyrnesli, N. Lorenzen, D. Otzen and E. E. Ferapontova, Analyst, 2014, 139, 749-756.
29. M. Vestergaard, K. Kerman, M. Saito, N. Nagatani, Y. Takamura and E. Tamiya, J Am Chem Soc, 2005, 127, 11892-11893.
30. C. J. Barrow and M. G. Zagorski, Science, 1991, 253, 179-182.
31. H. K. L. Blackley, G. H. W. Sanders, M. C. Davies, C. J. Roberts, S. J. B. Tendler and M. J. Wilkinson, J. Mol. Biol., 2000, 298, 833-840.
32. B. A. Chromy, R. J. Nowak, M. P. Lambert, K. L. Viola, L. Chang, P. T. Velasco, B. W. Jones, S. J. Fernandez, P. N. Lacor, P. Horowitz, C. E. Finch, G. A. Krafft and W. L. Klein, Biochemistry, 2003, 42, 12749-12760.
33. S. Shipovskov, A. M. Saunders, J. S. Nielsen, M. N. Hansen, K. V. Gothelf and E. E. Ferapontova, Biosens. Bioelectron., 2012, 37, 99-106.
34. E. E. Ferapontova, T. Ruzgas and L. Gorton, Anal. Chem., 2003, 75, 4841-4850.

